

Street-View Image Generation from a Bird’s-Eye View Layout

Alexander Swerdlow Runsheng Xu Bolei Zhou
 University of California, Los Angeles
 {aswerdlow, rxx3386}@ucla.edu, bolei@cs.ucla.edu

Abstract

Bird’s-Eye View (BEV) Perception has received increasing attention in recent years as it provides a concise and unified spatial representation across views and benefits a diverse set of downstream driving applications. While the focus has been placed on discriminative tasks such as BEV segmentation and detection, the dual generative task of creating street-view images from a BEV layout has been rarely explored. The ability to generate realistic street-view images that align with a given HD map and traffic layout is critical for visualizing complex traffic scenarios and developing robust perception models for autonomous driving. In this paper, we propose BEVGen, a conditional generative model that synthesizes a set of realistic and spatially consistent surrounding images that match the BEV layout of a traffic scenario. BEVGen incorporates a novel cross-view transformation with spatial attention design which learns the relationship between cameras and map views to ensure their consistency. We evaluate the proposed model on the challenging NuScenes and Argoverse 2 datasets. After training, BEVGen can accurately render road and lane lines, as well as generate traffic scenes under different weather conditions and times of day. The code is included in the supplement and will be made publicly available.

1. Introduction

BEV perception for autonomous driving is a fast-growing research topic, with the goal of learning a cross-view representation that transforms information between the perspective and bird’s-eye view. Such representation can be used in downstream tasks such as path planning and trajectory forecasting [1, 62]. The recent successes in BEV perception, whether for monocular images [10, 14, 15] or multi-view images [18, 56, 63], mostly focus on the discriminative side of BEV perception where the inputs are street-view images and the output is a semantic BEV layout. However, the generative side of BEV perception, which aims at synthesizing realistic street-view images from a given BEV semantic layout, is much less explored. A BEV layout concisely describes a

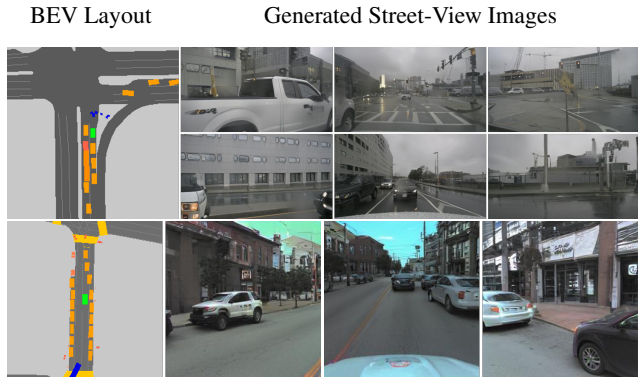


Figure 1. The proposed BEVGen generates realistic and spatially consistent street-view images from BEV layout. There are six camera views surrounding the ego vehicle as indicated by the green rectangle in the BEV layout. The two examples are generated by our model trained on NuScenes and Argoverse 2, respectively.

traffic scenario at the semantic level, therefore generating its corresponding street-view images can help visualize the scene in a more real-world setting.

There are many potential applications for the BEV generation task. For example, we can create synthetic training data for BEV segmentation models. Whereas most current approaches to synthetic training data involve a complex simulator or 3D reconstructed meshes, it is simpler to adopt a controllable generative model for diverse image generation. Another benefit provided by the BEV generation is the ease of visualizing and editing traffic scenes. In the case of self-driving vehicles, we often care about a small set of rare scenarios where an accident is likely to happen. Human users can intuitively edit a BEV layout and then use a generative model to output the corresponding street-view images for training or testing a driving system.

The fundamental question for BEV generation is: what could be a plausible set of street-view images that correspond to this BEV layout? One could think of numerous scenes with varying vehicle types, backgrounds, and more. For a set of views to be realistic, we need to consider several properties of the images. Similar to the problem of novel view

synthesis, images must appear consistent, as if they were taken in the same physical location. For instance, cameras with an overlapping field-of-view (FoV) should have overlapping content, and objects partially visible in one frame should appear in a rotated frame. The visual styling of the scene also needs to be consistent such that all virtual views appear to be created in the same geographical area (e.g., urban vs. rural), time of day, with the same weather conditions, and so on. In addition to image consistency, the images must correspond to the HD map, faithfully reproducing the specified road layout, lane lines, and vehicle locations. Unlike image-to-image translation with a semantic mask, the BEV generation model must infer the image layout to account for occlusions between objects and the relative heights of objects in a scene. These two main challenges, image consistency and correspondence, are critical to the task but can be difficult to reconcile. If we only desire image consistency, similar to the case of image outpainting, the model is free to generate any consistent image. However, if we also wish to maintain correspondence between the virtual views and the HD map, portions of the virtual views are constrained to represent certain elements (e.g., vehicles). On the other hand, if we only care about image correspondence, the model only needs the context of part of the HD map in its FoV and does not need to account for previously generated images or issues such as wraparound.

In this work, we tackle the new task of generating street-view images from a BEV layout and propose a generative model called BEVGen to address the underlying challenges. We develop an autoregressive neural model called BEVGen that generates a set of n realistic and spatially consistent images. Fig. 1 shows generation examples. BEVGen has two technical novelties: (i) it incorporates spatial embeddings using camera intrinsics and extrinsics to allow the model to attend to relevant portions of the images and HD map, and (ii) it contains a novel attention bias and decoding scheme that maintains both image consistency and correspondence. Thus the model can generate high-quality scenes with spatial awareness and scene consistency across camera views. Compared to baselines, the proposed model obtains substantial improvement in terms of image synthesis quality and semantic consistency. The model can also render realistic scene images from out-of-domain BEV maps, such as those provided by a driving simulator or edited by a user. We summarize our contributions as follows:

- We tackle the new task of multi-view image generation from BEV layout. It is the first attempt to explore the generative side of BEV perception for driving scenes.
- We develop a novel generative model BEVGen that can synthesize spatially consistent street-view images by incorporating spatial embeddings and a pairwise camera bias.
- The model achieves high-quality synthesis results and

shows promise for applications such as data augmentation and 3D simulation rendering.

2. Related Work

Cross-modal Image Generation. Cross-modal image generation has seen a lot of attention in recent years with work on text-to-image models [13, 36–38, 44], speech-to-image models [6, 21], and image-to-video models [46]. Others have focused on using more direct representations to control generation, including generation from semantic masks [19, 30, 58], or worked to convert higher-level representations such as text [16, 34], scene graphs [8, 20, 49, 57], and bounding boxes [24] into such a semantic mask. There have also been several attempts at learning spatially disentangled scene representations by composing latent features that correspond to specific parts of a scene [11, 31]. Our task is conceptually similar to image generation from a semantic mask but distinct in that our semantic representation only provides minimal layout constraints, lacking height information, direct occlusion representation, and background information.

Cross-view Synthesis. Several works have focused directly on the task of street-view synthesis from satellite views as a subset of the image-to-image translation problem [23, 27, 28, 39, 45, 48, 61]. These works are a form of image-to-image translation and commonly use a convolutional architecture for generation such as pix2pix [19] or cycleGAN [64]. These works attempt to tackle viewpoint transformation, from a top-down to an ego-centric view, that is implicitly required for our task, but unlike cross-view synthesis, our task does not benefit from the rich RGB representation provided by a satellite view. Furthermore, large portions of our virtual camera views, such as the side cameras, correspond to areas entirely unlabeled on our BEV map, and thus plausible semantics must be inferred from neighboring views and cannot simply be translated. We compare the representative work of cross-view synthesis in the later experiment section, the result is less ideal.

Image Outpainting. Spatial consistency is important for tasks such as image outpainting, where the goal is to generate or extend an image of the same scene. Early approaches for image outpainting used auto-regressive approaches on a pixel-wise level [7, 29, 50, 51]. However, this approach can be computationally expensive and thus is limited to generating low-resolution images. Subsequently, GANs were introduced to the task [17, 25, 43, 55] which do not suffer from the same computational limitations as pixel-wise autoregressive approaches. More recent works have utilized a Vector Quantised-Variational Autoencoder (VQ-VAE) [52] to great success [2, 4]. Similar to image outpainting, our task requires generated images to appear coherent in weather and location; however, we also seek to generate distinct, partially overlapping camera views and require that portions of these

views are conditionally generated from a BEV layout.

Novel View Synthesis. The same underlying VQ-VAE architecture has been used for the single-view novel view synthesis (NVS) task where the goal is to generate new virtual camera view given a source image. By conditioning an autoregressive transformer with camera translation and rotation, [42] showed that a transformer-based model can learn the 3D relationship between images without explicit depth maps or warping as used in prior attempts for single-view NVS such as in [41, 53]. To improve the consistency between frames, [40] suggests a camera-aware bias for self-attention that encodes the similarity between consecutive image frames. Our task requires a similar 3D understanding between different viewpoints as in NVS, but lacks the conditioning information provided by a source view(s) and requires consistency not only between frames but also with an HD map. If we broaden our task to allow for a source view, as we demonstrate in Fig. 8, our task can be thought of as a conditional NVS task.

3. Method

In this section, we introduce the framework of the proposed BEVGen. The problem definition of BEV generation is that given a semantic layout in Birds-Eye View (BEV), $B \in \mathbb{R}^{H_b \times W_b \times c_b}$ with the ego at the center and c_b channels describing the locations of vehicles, roads, lane lines, and more (see Sec. 4.1), we would like to generate n images $I_k \in \mathbb{R}^{H_c \times W_c \times 3}$ under a set of n virtual camera views $(K_k, R_k, t_k)_{k=1}^n$, where K_k, R_k, t_k are the intrinsics, extrinsic rotation, and translation of the k th camera.

Fig. 2 illustrates the framework of the proposed BEVGen. BEVGen consists of two autoencoders modeled by VQ-VAE, one for images and one for the BEV representation, that allow the causal transformer to model scenes at a high level. The key novelty lies in how the transformer can relate information between modalities and across different views. The cross-view transformation encodes a cross-modal inductive 3D bias, allowing the model to attend to relevant portions of the HD map and nearby image tokens. We explain each part in more detail below.

3.1. Model Structure

Image Encoder. To generate a globally coherent image, we model our distribution in a discrete latent space instead of pixel space. We use the VQ-VAE model introduced by Oord *et al.* [52] as an alternative generative architecture to GANs¹. We replace the L_2 with a perceptual loss and incorporate a patch-wise adversarial loss as in [12]. The VQ-VAE architecture consists of an encoder E^c , a decoder D^c , and a

¹Note that switching to the recently developed class of diffusion models can potentially improve the image synthesis quality, but such models require an order of magnitude of additional data and computational resources for training and thus we leave it for future works.

codebook $\mathcal{Z}^c = \{z_f\}_{f=1}^{F_c} \subset \mathbb{R}^{n_c}$ where F_c is the number of code vectors and n_c is the embedding dimension of each code. Given a source image, $x_k \in \mathbb{R}^{H_c \times W_c \times 3}$ we encode $\hat{z}_k^c = E^c(x_k) \in \mathbb{R}^{h_c \times w_c \times n_c}$. To obtain a discrete, tokenized representation, we find the nearest codebook vector for each feature vector $\hat{z}_{k,ij}^c \in \mathbb{R}^{n_c}$ where i, j are the row, column indices in the discrete latent representation with size $h_c \times w_c$:

$$z_{k,ij}^c = \arg \min_f \|\hat{z}_{k,ij}^c - z_f\| \in \mathbb{N}. \quad (1)$$

This creates a set of tokens $z_k^c \in \mathbb{N}^{h_c \times w_c}$ that we refer to as our image tokens. To generate an image from a set of tokens, we first obtain $\tilde{z}_k^c \in \mathbb{R}^{h_c \times w_c \times n_c}$, by using z_k^c as an index to our codebook, \mathcal{Z}^c . We decode with a convolutional decoder, $D^c(\tilde{z}_k^c) \in \mathbb{R}^{H_c \times W_c \times 3}$, using the same architecture as [12].

BEV Encoder. To condition our model on a BEV layout, we use a similar discrete representation as for camera images, except we replace the perceptual and adversarial losses with a binary cross entropy loss for binary channels and an L_2 loss for continuous channels. We encode our BEV map h as before with $E^b(h) \in \mathbb{R}^{h_b \times w_b \times n_b}$ and $\mathcal{Z}^b = \{z_f\}_{f=1}^{F_b} \subset \mathbb{R}^{n_b}$ to obtain a set of tokens, $z^b \in \mathbb{N}^{h_b \times w_b}$. We discard the decoder stage, D^b , after training the 1st stage as it is not needed for our second stage or for inference.

Autoregressive Modeling. Given a BEV layout and k sets of camera parameters, we seek to generate k images by learning the prior distribution of a set of discrete tokens, z conditioned on z^b, K, R, t .

$$p(z^c | z^b, K, R, t) = \prod_{i=0}^{h_c \times w_c \times k} p(z_i^c | z_{<i}^c, z^b, K, R, t). \quad (2)$$

We model $p(\cdot)$ by training a transformer τ that predicts the subsequent token based on the discretized BEV features, prior image tokens, and their respective camera parameters. We choose a transformer architecture as it provides global attention which aids in cross-view consistency.

3.2. Spatial Embeddings

To help the model attend to relevant tokens both in the camera and BEV feature space, we introduce positional embeddings. We take inspiration from work on BEV segmentation [63] on alignment between the BEV and first-person view (FPV) perspectives.

Camera Embedding. In order to align image tokens with BEV tokens, we use the known intrinsics and extrinsics to reproject from image coordinates to world coordinates. Given a token in image space, $z_{k,ij}^c$, we convert to homogeneous coordinates, $\tilde{z}_{k,ij}^c$ and obtain a direction vector in the ego frame as follows:

$$d_{k,ij} = R_k^{-1} K_k^{-1} \tilde{z}_{i,jk}^c + t_k. \quad (3)$$

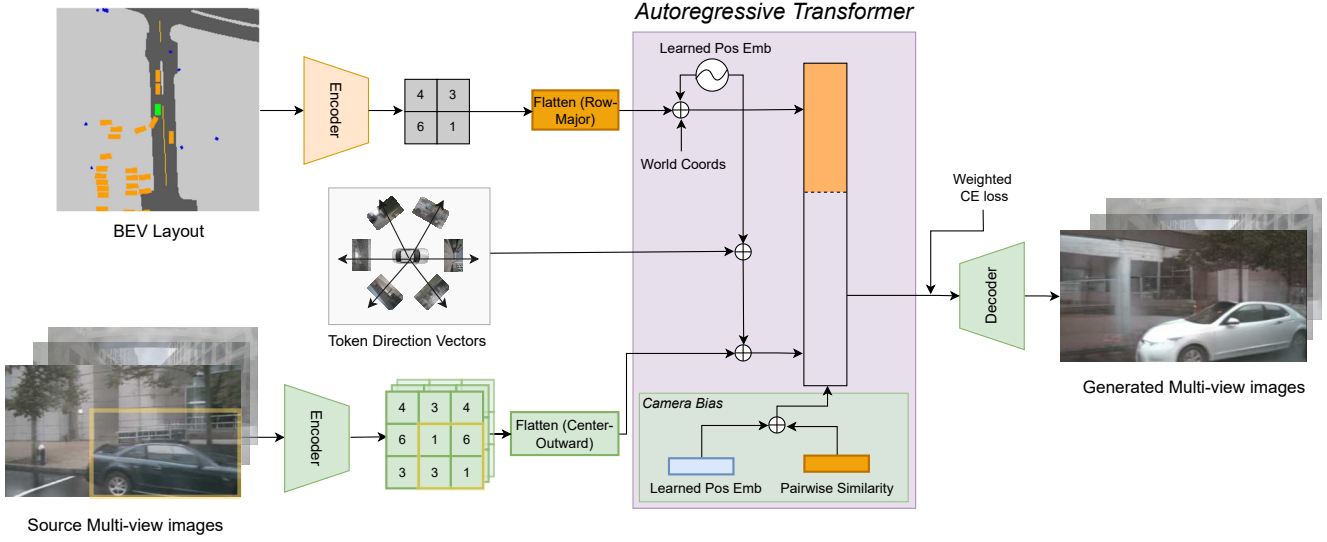


Figure 2. BEVGen framework. A BEV layout and source multi-view images are encoded to a discrete representation and are flattened before passed to the autoregressive transformer. Spatial embeddings are added to both camera and BEV tokens inside each transformed bloc, the learned pairwise camera bias are added to the attention weights. Weighted CE loss is applied during training, and we pass the tokens to the decoder to obtain generated images during inference.

We use a 1D convolution, $\theta_c(d) \in \mathbb{R}^{n \times h_c \times w_c \times n_{emb}}$, to encode our direction vector in the latent space of the transformer. We encode our image tokens using a shared learnable embedding $\lambda_c(z_{k,ij}^c) \in \mathbb{R}^{n_{emb}}$, and add a per-token learnable parameter, $\Lambda_{k,ij}^c \in \mathbb{R}^{n_{emb}}$, across image tokens:

$$l_{k,ij} = \lambda(z_{k,ij}^c) + \theta(d_{k,ij}) + \Lambda_{k,ij}. \quad (4)$$

BEV Embedding. To align our BEV tokens with our image tokens, we perform a similar operation as in Eq. (4) and use the known BEV layout dimensions to obtain coordinates in the ego frame, t_{xy} , for each token and encode these into our transformer latent space, with $\theta_b(t) \in \mathbb{R}^{h_b \times w_b \times n_{emb}}$. We similarly use a shared learnable embedding for our discrete tokens, $\lambda(z_{xy}^b) \in \mathbb{R}^{n_{emb}}$, and a per-token learnable parameter, Λ_{xy} :

$$l_{xy} = \lambda(z_{xy}^b) + \theta_b(t_{xy}) + \Lambda_{xy}. \quad (5)$$

, where l represents the final input embeddings for the transformer decoder block.

3.3. Camera Bias

In addition to providing the model with aligned embeddings, we add a bias to our self-attention layers that provides both an intramodal (image to image) and intermodal (image to BEV) similarity constraint. This draws inspiration from [40], but instead of providing a blockwise similarity matrix that is composed of encoded poses between frames, we provide a per-token similarity based on their relative direction vectors. Our approach also encodes the relationship

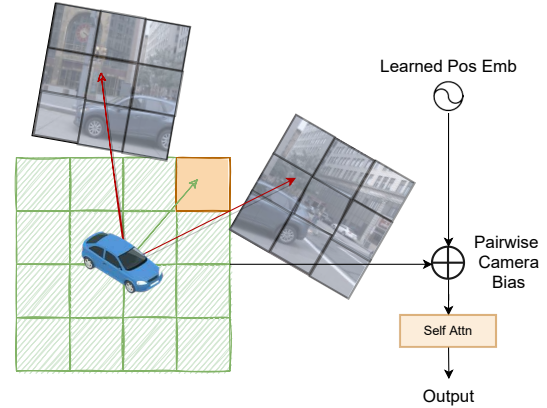


Figure 3. Camera Bias Overview. We construct a pairwise matrix that encodes relationship between a given image token and another BEV/image token.

between image and BEV tokens. For self-attention in any layer between some query q_r and key/value k_c/v_c we have:

$$\text{Attention}(q_r, k_c, v_c) = v_c \text{softmax} \left(\frac{a_{rc}}{\sqrt{d}} \right), \quad (6)$$

$$a_{rc} = q_r k_c + \beta_{rc}. \quad (7)$$

The transformer sequence is composed of $h_b w_b$ conditional BEV tokens followed by $h_c w_c$ camera tokens. If $r, c > h_b w_b$, both positions correspond to image tokens and thus we have two direction vectors, d_r, d_c , computed as in

Eq. (3). As discussed in Sec. 3.1, we have a mapping between the sequence index and image token (i, j) in camera k . If $r > h^b w^b > c$, we have a query for some image token and a key/value pair corresponding to BEV token. Thus, we again construct two direction vectors. In this case our BEV direction vector consists of the 2D World coordinates (in the ego-center frame) and our image direction vector is the same as in Eq. (3) except with the row value as the center of the image. Given these two direction vectors, d_r, d_c , we add the cosine similarity and a learnable parameter, θ_{rc} , as shown in Fig. 3:

$$\beta_{rc} = \frac{d_r \cdot d_c}{\|d_r\| \|d_c\|} + \theta_{rc}. \quad (8)$$

4. Experiments

4.1. Datasets

We evaluate the proposed method using the nuScenes dataset [3] and Argoverse 2 dataset [54], which are commonly used for BEV segmentation and detection. Each instance in both of our datasets contain ground-truth 3D bounding boxes, mutli-view camera images, calibrated camera intrinsics and extrinsics, and LiDAR. We project these 3D bounding boxes onto a BEV layout following standard practice used in BEV segmentation [18, 33, 63].

nuScenes. The nuScenes dataset provides full 360° camera coverage with a consistent camera resolution. nuScenes consists of 1000, 20-second scenes, captured at 12Hz by 6 Cameras, although synchronization occurs only at 12Hz. To increase our dataset size, we re-sample at 20Hz, pruning instances where any camera is more than 100ms outside of the frame. We linearly interpolate from the nearest ground-truth annotations to create paired annotation data. This provides roughly 9x the number of instances as the original training set, for a total of 260k instances. For validation, we use the standard set containing 6k instances. For all visualizations, we flip the back left and right cameras along the vertical axis to highlight the image consistency of our model.

Argoverse 2. Argoverse 2 comprises 1000, 15-second scenes annotated at 10hz, with a synchronized camera captured at 20hz. Compared to Argoverse 1 [5], it covers much broader and more diverse image content and is comparable to the size of nuScenes dataset. This provides 210k and 30k instances for train and validation, respectively. As the front camera is rotated 90°, we extract a square crop from the front three cameras for all experiments.

Preprocessing. The BEV layout representation used in training and testing covers $80m \times 80m$ around the ego center. On nuScenes, there are 21 channels, with 14 channels being binary masks representing map information (lane lines, dividers, etc.) and actor annotations (cars, trucks, pedestrians, etc.). The remaining 7 channels provide instance informa-

Method	FID↓	Road mIoU↑	Vehicle mIoU↑
X-Seq [39]	138.30	-	-
BEVGen	25.54	50.20	5.89
Sparse BEVGen	28.67	50.92	6.69

Table 1. Baseline Comparison over all 6 views on nuScenes Validation.

tion, including the visibility and size of the annotation. On nuScenes, we resize all images to $H \times W = 224 \times 400$, resulting in a discrete latent representation of $h_c \times w_c = 14 \times 25$. On Argoverse 2, we crop to $H \times W = 256 \times 256$, resulting in $h_c \times w_c = 16 \times 16$. Our BEV layout has a discrete latent representation of $h_b \times w_b = 16 \times 16$. We appropriately modify intrinsics after cropping and resizing. To enable our weighted cross-entropy loss, we project the provided 3D annotations onto the camera frame and weight the corresponding tokens in our discrete camera frame representation, $z_k \in \mathbb{N}^{h_c \times w_c}$.

4.2. Training Details

VQ-VAE. We train the 1st stage camera VQ-VAE with aggressive augmentation consisting of flips, rotations, color shifts, and crops. Similarly, we train our 1st stage BEV VQ-VAE with flips and rotations. For the 2nd stage, we add minimal rotations and scaling, as well as cropping.

Transformer. Our transformer is GPT-like [35] with 16-heads and 24-layers. We use DeepSpeed to facilitate sparse self-attention and 16-bit training. We clip gradients at 50 and use the AdamW optimizer [26] with $\beta_1, \beta_2 = 0.9, 0.95$ and a learning rate of $\lambda = 5e-7$. Both the BEV and image codebooks have $|\mathcal{Z}_c| = |\mathcal{Z}_b| = 1024$ codes with an embedding dimension, $n_c = n_b = 256$.

Additionally, we develop a lighter-weight model that uses sparse attention as in [9, 60]. As opposed to a uniform random attention mask, we unmask regions of the image near the token we attend. Using the same formulation as in Eq. (8), we create a pairwise similarity matrix for image tokens only. As sparse attention groups the input sequence into discrete blocks, we perform average pooling on these blocks and use these values as weights for sampling. Additionally, we have a sliding window in which we always attend to the last r tokens, and we attend to all BEV tokens. For our sparse models, we have an attention mask density of 35% with a sliding window length of $r = 96$. Except as described in Sec. 4.4, our sparse model is derived from fine-tuning our full-attention model for 10 epochs.

4.3. Results

Qualitative result. Fig. 4 exhibits the generation examples from BEVGen on nuScenes. Our model is able to generate

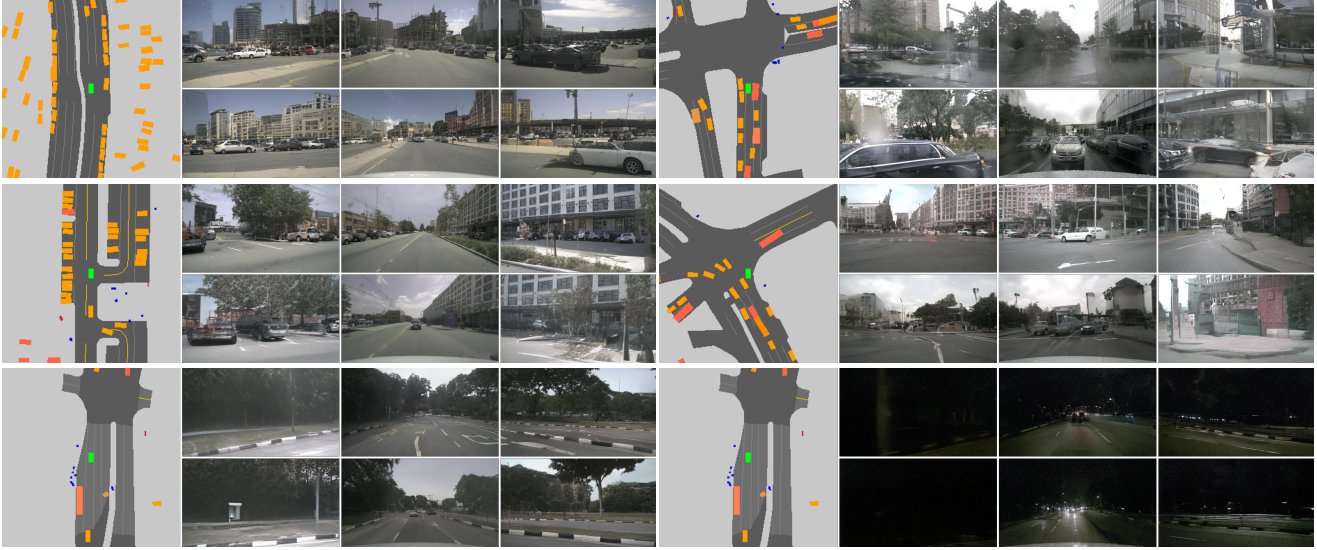


Figure 4. Synthesized multi-view images from BEVGen on nuScenes. Image contents are diverse and realistic. The two instances in the bottom row use the same BEV layout for synthesizing the same location in day and night.

a diverse set of scenes including intersections, parking lots, and boulevards. We observe that each camera view not only correctly displays the surrounding of the same location, but also preserves the spatial perspective. BEVGen synthesizes images under various weather conditions, with the same weather apparent in all images, including physical artifacts such as rain. We also demonstrate that our model is capable of generating diverse scenes corresponding to the same BEV layout. We see at the bottom of Fig. 4 the same location rendered in the day and at night by the model.

In Fig. 5, we compare synthesized images to real ones for the same BEV layouts on Argoverse 2. We observe that our model places vehicles in the same location as the real one, even when a vehicle is in multiple views. This demonstrates that the model learns to synthesize coherent content across views.

Quantitative result. We use the Fréchet Inception Distance (FID) to evaluate our synthesized quality compared to the source images. Metrics are calculated on the validation set for each respective dataset. We employ no post-generation filtering. For calculating FID scores, we use clean-fid [32].

To differentiate between the performance of our 1st and 2nd stage, we compare our results to the results obtained by feeding the encoded tokens directly to the decoder, as is done when training the 1st stage. This represents the theoretical upper bound of our model’s performance, largely removing the effect of the 1st stage which is not the focus of this paper.

As seen in Table 1, our BEVGen model achieved an FID score of 25.54 on nuScenes, compared to the baseline score of 138.30. This is in comparison to our reference upper-bound FID score of 9.37. Our model utilizing our sparse masking design from Sec. 3.4 achieved an FID score of

28.67. This sparse variant is approximately 48% faster during inference and 40% faster for training. On Argoverse 2, our model achieves an FID score of 25.51.

While FID is a common metric to measure image synthesis quality, it fails to entirely capture the design goals of our task and cannot reflect the synthesis quality of different semantic categories. Since we seek to generate multi-view images consistent with a BEV layout, we wish to measure our performance on this consistency. To do this, we leverage a pre-trained BEV segmentation network CVT from [63]. We apply the CVT to the generated images and then compare the predicted layout with the ground-truth BEV layout. We report both the road and vehicle class mean intersection-over-union (mIoU) scores. Note that the performance of the BEV segmentation model on the validation set is 66.31 and 27.51 for road and vehicle mIoU respectively. This reveals that though the model can generate road regions in the image in a reasonable manner, it still has a limited capability of generating high-quality individual vehicles that can be recognized correctly by the segmentation network. This is a common problem for scene generation where it remains challenging to synthesize the small objects entirely. Our work is a starting point and we plan to improve small object synthesis in future work.

Finally, we seek to quantitatively verify the cross-view consistency of our model. To do this, we introduce a consistency metric that looks at the similarity between overlapping portions of images. For example, for the front-left and front-center camera on nuScenes, we extract a window on the right and left edges of the images, respectively. We then attempt to find keypoint correspondences between these image patches by performing feature matching with [47]. As each



Figure 5. Comparison to real-views on Argoverse 2. Images on the left are synthesized, images on the right are corresponding real ones.



Figure 6. We display correspondences across views. Green lines indicate inliers obtained using RANSAC for filtering. Left: Real images, Right: Synthesized images.



Figure 7. Comparison to cross-view synthesis method. From left to right: BEVGen result, BEV layout, Predicted Street-View Segmentation mask from BEV, X-Seq [39] result.

correspondence has a confidence, we simply find the sum of these confidences and average across all windows to obtain a metric for cross-view consistency. We call this metric the View Consistency Score (VSC). On nuScenes, synthesized view images from our model obtain a VSC of 5.65, with the corresponding real images obtaining a result of 12.86. On Argoverse 2, synthesized view images obtain a VSC of 13.00, with the corresponding real images obtaining a result of 42.90. We see ablations for this metric in Table 2. We show the matched keypoints across views in Fig. 6.

As far as we know, our work is the first attempt at synthesizing street views conditioned on a BEV layout. To establish a comparison baseline, we reproduce one of the cross-view synthesis methods proposed in [39]. Firstly, we project the BEV semantic mask onto the camera perspective view using extrinsics and intrinsics. Next, we utilize a conditional GAN

to generate a street view semantic mask from this warped BEV layout. Finally, we use another conditional GAN to perform the semantic mask-to-image translation. As neither the nuScenes nor the Argoverse datasets provide 2D segmentation labels, we use a pre-trained segmentation model [59] to generate pseudo ground-truth labels for the first conditional GAN. Following [39], we use the Pix2Pix [19] model for the first and second stage. We compare the generation quality of BEVGen to this baseline, using the same BEV layout in Fig. 7. We see that BEVGen synthesized street images with much higher quality.

View-conditioned generation. We test the ability of our model to synthesize other views when provided a view from a single camera as seen in Fig. 8. We observe that our model is able to generate consistent imagery both in scene content and time of day.

4.4. Ablation Study

To verify the effectiveness of our design choices, we run an ablation study on key features of our model. We run these experiments on the same subset of the nuScenes validation set as in Sec. 4.3, but only consider the 3 front-facing views to reduce training time. The 3 front-facing views have a larger FoV overlap and capture more relevant scene features compared to the side-facing rear views. This is more relevant to our task as it allows us to better verify the design objectives of our model.

We test four variants of our model, one with only center-out decoding, one with our camera bias, one with the camera bias and spatial embeddings, and a final model that we train from scratch using our sparse masking, instead of fine-tuning. Table 2 shows a steady decrease in FID scores and increase in VSC, as we add the camera bias, and spatial embeddings.

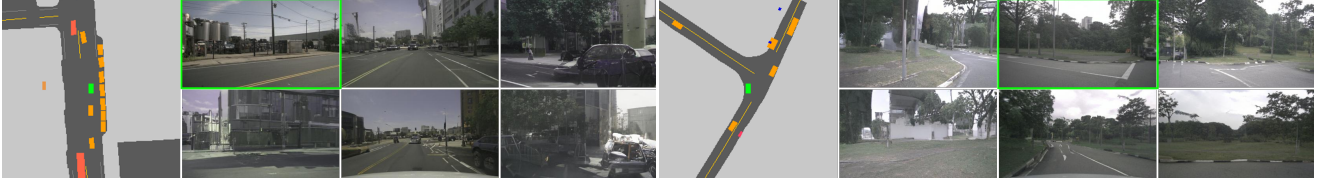


Figure 8. View-conditioned generation on nuScenes. Green box indicates the provided source tokens.



Figure 9. Generating images based on the BEV layouts provided by the MetaDrive driving simulator

Method	FID↓	VSC↑
Row-major Decoding	43.18	4.33
Center-out Decoding	42.32	4.53
+ Camera Bias	41.20	4.74
+ Camera Bias, Spatial Embedding	40.48	6.24
+ Sparse, Camera Bias, Spatial Embedding	48.31	5.44

Table 2. Ablation of the key model components.

	Road mIoU	Vehicle mIoU
CVT (w/o augmentation)	71.3	36.0
CVT (w/ augmentation)	71.9	36.6

Table 3. Application of data augmentation. We report the segmentation results on the validation set of nuScenes trained from the original training set and the one augmented with synthetic data.

5. Applications

Generating realistic images from BEV layout has many applications. In this section we explore the applications of data augmentation for BEV segmentation and image generation from simulated BEV.

Data augmentation for BEV segmentation. An important application of our BEV conditional generative model is generating synthetic data to improve prediction models. Thus, we seek to verify the effectiveness of our model by incorporating our generated images as augmented samples during training of a BEV segmentation model. We use CVT [63] as our model, which is also used in Sec. 4.3, and compare our results to training without any synthetic samples. We generate 6,000 unique instances using the BEV layout from the *train* set on nuScenes. These synthetic instances are associated with the ground truth BEV layout for training, with

no relation to results from Sec. 4.3. To reduce the effect of randomness during training, we set the random seed and disable non-deterministic operations for all training. As seen in Table 3, our data improves validation mIoU by 0.6 for both the road category and the vehicle category.

Image generation from simulated BEV. Since one motivation for our task definition lies in the simplicity of the BEV layout, we wish to determine whether this enables our model to generate new scenes from out-of-domain (OOD) HD maps. We use MetaDrive simulator [22] to generate random traffic scenarios and their associated BEV layouts in simulation, and then input the BEV layouts in our BEVGen. Generated images are shown in Fig. 9. We can see that our model can turn the simulated scenes into realistic street images using the BEV layout as a bridge. It has potential to address the sim2real gap.

6. Conclusion

In this work we tackle the BEV generation task by developing a generative model called BEVGen. After training on real-world driving dataset, the proposed model can generate spatially consistent multi-view images from a given BEV layout. We further show its application on data augmentation and simulated BEV generation.

Limitations and Future work. Future work may focus on both generation quality as well as consistency for smaller objects such as pedestrians. Replacing the encoder with a diffusion model may further improve the image synthesis quality. Furthermore, we plan to decouple the generation of foreground and background to address this issue in future work.

References

- [1] Adil Kaan Akan and Fatma Güney. StretchBEV: Stretching Future Instance Prediction Spatially and Temporally. In Shai

- Avidan, Gabriel J. Brostow, Moustapha Cissé, Giovanni Maria Farinella, and Tal Hassner, editors, *Computer Vision - ECCV 2022 - 17th European Conference, Tel Aviv, Israel, October 23-27, 2022, Proceedings, Part XXXVIII*, volume 13698 of *Lecture Notes in Computer Science*, pages 444–460, 2022. 1
- [2] Naofumi Akimoto, Yuhi Matsuo, and Yoshimitsu Aoki. Diverse Plausible 360-Degree Image Outpainting for Efficient 3DCG Background Creation. In *Proceedings of the IEEE/CVF Conference on Computer Vision and Pattern Recognition*, pages 11441–11450, 2022. 2
- [3] Holger Caesar, Varun Bankiti, Alex H. Lang, Sourabh Vora, Venice Erin Liong, Qiang Xu, Anush Krishnan, Yu Pan, Giancarlo Baldan, and Oscar Beijbom. nuScenes: A Multimodal Dataset for Autonomous Driving. In *2020 IEEE/CVF Conference on Computer Vision and Pattern Recognition (CVPR)*, pages 11618–11628, June 2020. 5
- [4] Huiwen Chang, Han Zhang, Lu Jiang, Ce Liu, and William T. Freeman. MaskGIT: Masked Generative Image Transformer. In *2022 IEEE/CVF Conference on Computer Vision and Pattern Recognition (CVPR)*, pages 11305–11315, June 2022. 2
- [5] Ming-Fang Chang, John Lambert, Patsorn Sangkloy, Jagjeet Singh, Slawomir Bak, Andrew Hartnett, De Wang, Peter Carr, Simon Lucey, Deva Ramanan, and James Hays. Argoverse: 3D Tracking and Forecasting With Rich Maps. In *Proceedings of the IEEE/CVF Conference on Computer Vision and Pattern Recognition*, pages 8748–8757, 2019. 5
- [6] Lele Chen, Sudhanshu Srivastava, Zhiyao Duan, and Chenliang Xu. Deep Cross-Modal Audio-Visual Generation. In *Proceedings of the on Thematic Workshops of ACM Multimedia 2017*, Thematic Workshops '17, pages 349–357, New York, NY, USA, Oct. 2017. 2
- [7] Mark Chen, Alec Radford, Rewon Child, Jeffrey Wu, Heewoo Jun, David Luan, and Ilya Sutskever. Generative Pretraining From Pixels. In *Proceedings of the 37th International Conference on Machine Learning*, pages 1691–1703, Nov. 2020. 2
- [8] Helisa Dhama, Azade Farshad, Iro Laina, Nassir Navab, Gregory D. Hager, Federico Tombari, and Christian Rupprecht. Semantic Image Manipulation Using Scene Graphs. In *Proceedings of the IEEE/CVF Conference on Computer Vision and Pattern Recognition*, pages 5213–5222, 2020. 2
- [9] Ming Ding, Zhuoyi Yang, Wenyi Hong, Wendi Zheng, Chang Zhou, Da Yin, Junyang Lin, Xu Zou, Zhou Shao, Hongxia Yang, and Jie Tang. CogView: Mastering Text-to-Image Generation via Transformers. In *Advances in Neural Information Processing Systems*, volume 34, pages 19822–19835, 2021. 5
- [10] Pramit Dutta, Ganesh Sistu, Senthil Yogamani, Edgar Galván, and John McDonald. ViT-BEVSeg: A Hierarchical Transformer Network for Monocular Birds-Eye-View Segmentation. In *2022 International Joint Conference on Neural Networks (IJCNN)*, pages 1–7, July 2022. 1
- [11] Dave Epstein, Taesung Park, Richard Zhang, Eli Shechtman, and Alexei A. Efros. BlobGAN: Spatially disentangled scene representations. *European Conference on Computer Vision (ECCV)*, 2022. 2
- [12] Patrick Esser, Robin Rombach, and Björn Ommer. Taming Transformers for High-Resolution Image Synthesis. In *2021 IEEE/CVF Conference on Computer Vision and Pattern Recognition (CVPR)*, pages 12868–12878, June 2021. 3
- [13] Oran Gafni, Adam Polyak, Oron Ashual, Shelly Sheynin, Devi Parikh, and Yaniv Taigman. Make-A-Scene: Scene-Based Text-to-Image Generation with Human Priors. In Shai Avidan, Gabriel J. Brostow, Moustapha Cissé, Giovanni Maria Farinella, and Tal Hassner, editors, *Computer Vision - ECCV 2022 - 17th European Conference, Tel Aviv, Israel, October 23-27, 2022, Proceedings, Part XV*, volume 13675 of *Lecture Notes in Computer Science*, pages 89–106, 2022. 2
- [14] Shi Gong, Xiaoqing Ye, Xiao Tan, Jingdong Wang, Errui Ding, Yu Zhou, and Xiang Bai. GitNet: Geometric Prior-Based Transformation for Birds-Eye-View Segmentation. In Shai Avidan, Gabriel J. Brostow, Moustapha Cissé, Giovanni Maria Farinella, and Tal Hassner, editors, *Computer Vision - ECCV 2022 - 17th European Conference, Tel Aviv, Israel, October 23-27, 2022, Proceedings, Part I*, volume 13661 of *Lecture Notes in Computer Science*, pages 396–411, 2022. 1
- [15] Nikhil Gosala and Abhinav Valada. Bird’s-Eye-View Panoptic Segmentation Using Monocular Frontal View Images. *IEEE Robotics and Automation Letters*, 7(2):1968–1975, Apr. 2022. 1
- [16] Seunghoon Hong, Dingdong Yang, Jongwook Choi, and Honglak Lee. Inferring Semantic Layout for Hierarchical Text-to-Image Synthesis. In *2018 IEEE/CVF Conference on Computer Vision and Pattern Recognition*, pages 7986–7994, Salt Lake City, UT, USA, June 2018. 2
- [17] Basile Van Hoorick. Image Outpainting and Harmonization using Generative Adversarial Networks. *CoRR*, abs/1912.10960, 2019. 2
- [18] Anthony Hu, Zak Murez, Nikhil Mohan, Sofia Dudas, Jeffrey Hawke, Vijay Badrinarayanan, Roberto Cipolla, and Alex Kendall. FIERY: Future Instance Prediction in Bird’s-Eye View From Surround Monocular Cameras. In *Proceedings of the IEEE/CVF International Conference on Computer Vision*, pages 15273–15282, 2021. 1, 5
- [19] Phillip Isola, Jun-Yan Zhu, Tinghui Zhou, and Alexei A. Efros. Image-To-Image Translation With Conditional Adversarial Networks. In *Proceedings of the IEEE Conference on Computer Vision and Pattern Recognition*, pages 1125–1134, 2017. 2, 7
- [20] Justin Johnson, Agrim Gupta, and Li Fei-Fei. Image Generation from Scene Graphs. In *2018 IEEE/CVF Conference on Computer Vision and Pattern Recognition*, pages 1219–1228, June 2018. 2
- [21] Jiguo Li, Xinfeng Zhang, Chuanmin Jia, Jizheng Xu, Li Zhang, Yue Wang, Siwei Ma, and Wen Gao. Direct Speech-to-image Translation. *IEEE J. Sel. Top. Signal Process.*, 14(3):517–529, Mar. 2020. 2
- [22] Quanyi Li, Zhenghao Peng, Lan Feng, Qihang Zhang, Zhenghai Xue, and Bolei Zhou. Metadrive: Composing diverse driving scenarios for generalizable reinforcement learning. *IEEE Transactions on Pattern Analysis and Machine Intelligence*, 2022. 8
- [23] Zuoyue Li, Zhenqiang Li, Zhaopeng Cui, Rongjun Qin, Marc Pollefeys, and Martin R. Oswald. Sat2Vid: Street-view

- Panoramic Video Synthesis from a Single Satellite Image. In *2021 IEEE/CVF International Conference on Computer Vision (ICCV)*, pages 12416–12425, Montreal, QC, Canada, Oct. 2021. [2](#)
- [24] Zejian Li, Jingyu Wu, Immanuel Koh, Yongchuan Tang, and Lingyun Sun. Image Synthesis from Layout with Locality-Aware Mask Adaption. In *2021 IEEE/CVF International Conference on Computer Vision (ICCV)*, pages 13799–13808, Montreal, QC, Canada, Oct. 2021. [2](#)
- [25] Han Lin, Maurice Pagnucco, and Yang Song. Edge Guided Progressively Generative Image Outpainting. In *2021 IEEE/CVF Conference on Computer Vision and Pattern Recognition Workshops (CVPRW)*, pages 806–815, Nashville, TN, USA, June 2021. [2](#)
- [26] Ilya Loshchilov and Frank Hutter. Decoupled Weight Decay Regularization, Jan. 2019. [5](#)
- [27] Xiaohu Lu, Zuoyue Li, Zhaopeng Cui, Martin R. Oswald, Marc Pollefeys, and Rongjun Qin. Geometry-Aware Satellite-to-Ground Image Synthesis for Urban Areas. In *2020 IEEE/CVF Conference on Computer Vision and Pattern Recognition (CVPR)*, pages 856–864, June 2020. [2](#)
- [28] Arun Mallya, Ting-Chun Wang, Karan Sapra, and Ming-Yu Liu. World-Consistent Video-to-Video Synthesis, July 2020. [2](#)
- [29] Jacob Menick and Nal Kalchbrenner. Generating High Fidelity Images with Subscale Pixel Networks and Multidimensional Upscaling. In *International Conference on Learning Representations*, 2019. [2](#)
- [30] Sangwoo Mo, Minsu Cho, and Jinwoo Shin. InstaGAN: Instance-aware Image-to-Image Translation. *CoRR*, abs/1812.10889, 2018. [2](#)
- [31] Thu H Nguyen-Phuoc, Christian Richardt, Long Mai, Yongliang Yang, and Niloy Mitra. BlockGAN: Learning 3D Object-aware Scene Representations from Unlabelled Images. In *Advances in Neural Information Processing Systems*, volume 33, pages 6767–6778, 2020. [2](#)
- [32] Gaurav Parmar, Richard Zhang, and Jun-Yan Zhu. On aliased resizing and surprising subtleties in GAN evaluation. In *CVPR*, 2022. [6](#)
- [33] Jonah Philion and Sanja Fidler. Lift, Splat, Shoot: Encoding Images from Arbitrary Camera Rigs by Implicitly Unprojecting to 3D. In Andrea Vedaldi, Horst Bischof, Thomas Brox, and Jan-Michael Frahm, editors, *Computer Vision – ECCV 2020*, Lecture Notes in Computer Science, pages 194–210, Cham, 2020. [5](#)
- [34] Tingting Qiao, Jing Zhang, Duanqing Xu, and Dacheng Tao. Learn, Imagine and Create: Text-to-Image Generation from Prior Knowledge. In *Advances in Neural Information Processing Systems*, volume 32, 2019. [2](#)
- [35] Alec Radford, Jeffrey Wu, Rewon Child, David Luan, Dario Amodei, and Ilya Sutskever. Language Models are Unsupervised Multitask Learners. page 24. [5](#)
- [36] Aditya Ramesh, Prafulla Dhariwal, Alex Nichol, Casey Chu, and Mark Chen. Hierarchical Text-Conditional Image Generation with CLIP Latents. *CoRR*, abs/2204.06125, 2022. [2](#)
- [37] Aditya Ramesh, Mikhail Pavlov, Gabriel Goh, Scott Gray, Chelsea Voss, Alec Radford, Mark Chen, and Ilya Sutskever. Zero-Shot Text-to-Image Generation. In *Proceedings of the 38th International Conference on Machine Learning*, pages 8821–8831, July 2021. [2](#)
- [38] Scott Reed, Zeynep Akata, Xinchun Yan, Lajanugen Logeswaran, Bernt Schiele, and Honglak Lee. Generative Adversarial Text to Image Synthesis. In *Proceedings of The 33rd International Conference on Machine Learning*, pages 1060–1069, June 2016. [2](#)
- [39] Krishna Regmi and Ali Borji. Cross-View Image Synthesis Using Conditional GANs. In *2018 IEEE/CVF Conference on Computer Vision and Pattern Recognition*, pages 3501–3510, Salt Lake City, UT, USA, June 2018. [2](#), [5](#), [7](#)
- [40] Xuanchi Ren and Xiaolong Wang. Look Outside the Room: Synthesizing A Consistent Long-Term 3D Scene Video from A Single Image. In *2022 IEEE/CVF Conference on Computer Vision and Pattern Recognition (CVPR)*, pages 3553–3563, New Orleans, LA, USA, June 2022. [3](#), [4](#)
- [41] Chris Rockwell, David F. Fouhey, and Justin Johnson. Pixel-Synth: Generating a 3D-Consistent Experience From a Single Image. In *Proceedings of the IEEE/CVF International Conference on Computer Vision*, pages 14104–14113, 2021. [3](#)
- [42] Robin Rombach, Patrick Esser, and Bjorn Ommer. Geometry-Free View Synthesis: Transformers and no 3D Priors. In *2021 IEEE/CVF International Conference on Computer Vision (ICCV)*, pages 14336–14346, Montreal, QC, Canada, Oct. 2021. [3](#)
- [43] Mark Sabini and Gili Rusak. Painting Outside the Box: Image Outpainting with GANs. *CoRR*, abs/1808.08483, 2018. [2](#)
- [44] Chitwan Saharia, William Chan, Saurabh Saxena, Lala Li, Jay Whang, Emily Denton, Seyed Kamyar Seyed Ghasemipour, Burcu Karagol Ayan, S. Sara Mahdavi, Rapha Gontijo Lopes, Tim Salimans, Jonathan Ho, David J. Fleet, and Mohammad Norouzi. Photorealistic Text-to-Image Diffusion Models with Deep Language Understanding. *CoRR*, abs/2205.11487, 2022. [2](#)
- [45] Yujiao Shi, Dylan Campbell, Xin Yu, and Hongdong Li. Geometry-Guided Street-View Panorama Synthesis From Satellite Imagery. *IEEE Transactions on Pattern Analysis and Machine Intelligence*, 44(12):10009–10022, Dec. 2022. [2](#)
- [46] Uriel Singer, Adam Polyak, Thomas Hayes, Xi Yin, Jie An, Songyang Zhang, Qiyuan Hu, Harry Yang, Oron Ashual, Oran Gafni, Devi Parikh, Sonal Gupta, and Yaniv Taigman. Make-A-Video: Text-to-Video Generation without Text-Video Data. *CoRR*, abs/2209.14792, 2022. [2](#)
- [47] Jiaming Sun, Zehong Shen, Yuang Wang, Hujun Bao, and Xiaowei Zhou. LoFTR: Detector-Free Local Feature Matching With Transformers. In *IEEE Conference on Computer Vision and Pattern Recognition, CVPR 2021, Virtual, June 19-25, 2021*, pages 8922–8931, 2021. [6](#)
- [48] Aysim Toker, Qunjie Zhou, Maxim Maximov, and Laura Leal-Taixe. Coming Down to Earth: Satellite-to-Street View Synthesis for Geo-Localization. In *2021 IEEE/CVF Conference on Computer Vision and Pattern Recognition (CVPR)*, pages 6484–6493, Nashville, TN, USA, June 2021. [2](#)
- [49] Subarna Tripathi, Anahita Bhiwandiwala, Alexei Bastidas, and Hanlin Tang. Using Scene Graph Context to Improve Image Generation. *CoRR*, abs/1901.03762, 2019. [2](#)

- [50] Aaron van den Oord, Nal Kalchbrenner, Lasse Espeholt, koray kavukcuoglu, Oriol Vinyals, and Alex Graves. Conditional Image Generation with PixelCNN Decoders. In *Advances in Neural Information Processing Systems*, volume 29, 2016. 2
- [51] Aäron van den Oord, Nal Kalchbrenner, and Koray Kavukcuoglu. Pixel Recurrent Neural Networks. In *Proceedings of The 33rd International Conference on Machine Learning*, pages 1747–1756, June 2016. 2
- [52] Aaron van den Oord, Oriol Vinyals, and koray kavukcuoglu. Neural Discrete Representation Learning. In *Advances in Neural Information Processing Systems*, volume 30, 2017. 2, 3
- [53] Olivia Wiles, Georgia Gkioxari, Richard Szeliski, and Justin Johnson. SynSin: End-to-End View Synthesis From a Single Image. In *2020 IEEE/CVF Conference on Computer Vision and Pattern Recognition (CVPR)*, pages 7465–7475, Seattle, WA, USA, June 2020. 3
- [54] Benjamin Wilson, William Qi, Tanmay Agarwal, John Lambert, Jagjeet Singh, Siddhesh Khandelwal, Bowen Pan, Ratnesh Kumar, Andrew Hartnett, Jhony Kaesemodel Pontes, Deva Ramanan, Peter Carr, and James Hays. Argoverse 2: Next Generation Datasets for Self-Driving Perception and Forecasting. In Joaquin Vanschoren and Sai-Kit Yeung, editors, *Proceedings of the Neural Information Processing Systems*, 2021. 5
- [55] Qingguo Xiao, Guangyao Li, and Qiaochuan Chen. Image Outpainting: Hallucinating Beyond the Image. *IEEE Access*, 8:173576–173583, 2020. 2
- [56] Runsheng Xu, Zhengzhong Tu, Hao Xiang, Wei Shao, Bolei Zhou, and Jiaqi Ma. CoBEVT: Cooperative bird’s eye view semantic segmentation with sparse transformers. In *Conference on Robot Learning (CoRL)*, 2022. 1
- [57] Chiao-An Yang, Cheng-Yo Tan, Wan-Cyuan Fan, Cheng-Fu Yang, Meng-Lin Wu, and Yu-Chiang Frank Wang. Scene Graph Expansion for Semantics-Guided Image Outpainting. In *2022 IEEE/CVF Conference on Computer Vision and Pattern Recognition (CVPR)*, pages 15596–15605, New Orleans, LA, USA, June 2022. 2
- [58] Yurong You, Xinlei Pan, Ziyang Wang, and Cewu Lu. Virtual to Real Reinforcement Learning for Autonomous Driving. *CoRR*, abs/1704.03952, 2017. 2
- [59] Yuhui Yuan, Xilin Chen, and Jingdong Wang. Object-Contextual Representations for Semantic Segmentation. In Andrea Vedaldi, Horst Bischof, Thomas Brox, and Jan-Michael Frahm, editors, *Computer Vision - ECCV 2020 - 16th European Conference, Glasgow, UK, August 23-28, 2020, Proceedings, Part VI*, volume 12351 of *Lecture Notes in Computer Science*, pages 173–190, 2020. 7
- [60] Manzil Zaheer, Guru Guruganesh, Kumar Avinava Dubey, Joshua Ainslie, Chris Alberti, Santiago Ontanon, Philip Pham, Anirudh Ravula, Qifan Wang, Li Yang, and Amr Ahmed. Big Bird: Transformers for Longer Sequences. In *Advances in Neural Information Processing Systems*, volume 33, pages 17283–17297, 2020. 5
- [61] Menghua Zhai, Zachary Bessinger, Scott Workman, and Nathan Jacobs. Predicting Ground-Level Scene Layout from Aerial Imagery. In *2017 IEEE Conference on Computer Vision and Pattern Recognition (CVPR)*, pages 4132–4140, Honolulu, HI, July 2017. 2
- [62] Yunpeng Zhang, Zheng Zhu, Wenzhao Zheng, Junjie Huang, Guan Huang, Jie Zhou, and Jiwen Lu. BEVerse: Unified Perception and Prediction in Birds-Eye-View for Vision-Centric Autonomous Driving. *CoRR*, abs/2205.09743, 2022. 1
- [63] Brady Zhou and Philipp Krähenbühl. Cross-view Transformers for real-time Map-view Semantic Segmentation. In *2022 IEEE/CVF Conference on Computer Vision and Pattern Recognition (CVPR)*, pages 13750–13759, June 2022. 1, 3, 5, 6, 8
- [64] Jun-Yan Zhu, Taesung Park, Phillip Isola, and Alexei A. Efros. Unpaired Image-to-Image Translation Using Cycle-Consistent Adversarial Networks. In *2017 IEEE International Conference on Computer Vision (ICCV)*, pages 2242–2251, Venice, Oct. 2017. 2